LA-UR- 98-2644

Approved for public release; distribution is unlimited.

Title: Space Charge in Proton Linacs

CONF-980567--

Author(s): T. P. Wangler
F. E. Merrill
L. J. Rybarcyk
R. D. Ryne

Submitted to: Space Charge Physics in High Intensity Hadron Rings
Long Island, NY
5/4-7/98

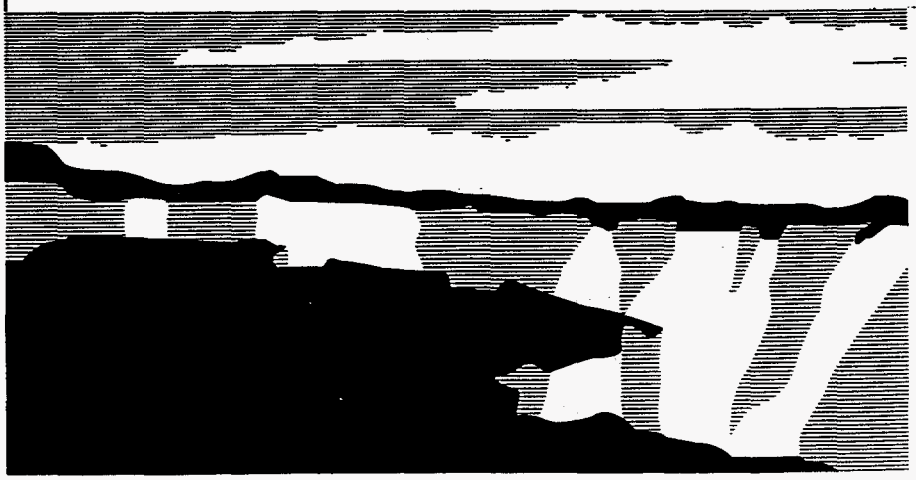

Los Alamos
NATIONAL LABORATORY

DISCLAIMER

DISCLAIMER

Portions of this document may be illegible in electronic image products. Images are produced from the best available original document.

LA-UR- 98-2644

SPACE CHARGE IN PROTON LINACS

T.P.Wangler, F. Merrill, L. Rybarcyk, and R. Ryne

Los Alamos National Laboratory

1. Introduction

There are at least two reasons why we may be interested in space-charge effects in proton linacs at this workshop. First, we can expect that there are some areas of commonality in the space-charge physics of linacs and circular machines. Second, a linac delivers the input beam to a circular machine, so understanding the linac physics helps to explain the limitations for the input beam quality to a ring. This presentation is divided into three parts. First, we discuss space-charge effects from the linac point of view. Second, we discuss practical methods of calculation of linac beam dynamics that include space-charge forces. Finally, we summarize the status of experimental studies of the beam performance in the LANSCE linac including space-charge effects.

2. Space Charge from the Linac Viewpoint

We begin by reviewing the characteristics of space-charge forces in accelerator beams. A smooth space-charge potential is generally used to replace the actual Coulomb interactions of the particles in the beam. This is a good approximation when the number of particles in a sphere with radius equal to the Debye length is much larger than unity. This is usually true for beams in linacs and rings; in high current linacs the number of particles in a Debye sphere is typically of order 10^6. Even with this approximation, the space-charge force does not have simple properties. In general it is nonlinear, time dependent, coupled in x, y, and z, and exhibits effects that are common in plasma physics such as collective oscillations and Debye shielding.

In a proton linac the space-charge force can have major consequences on the beam dynamics. First, the beam current is limited by the space-charge force in both the longitudinal and transverse directions. The value of the matched rms beam size is determined by a balance between the defocusing effects of emittance and space charge, and the focusing effect of the external forces. If the beam current increases and all other parameters remain constant, the rms beam size will increase. In the

transverse direction the aperture limits the growth of the beam size and sets the transverse current limit. In the longitudinal direction the beam size is limited by the phase width of the rf separatrix, which sets the longitudinal current limit. Assuming that the bunch density is uniform, the space-charge force is a linear function of displacement from the bunch center. Then analytic formulas can be derived for these current limits.

If the bunch density is nonuniform, the space-charge fields are nonlinear. Under these conditions the nonlinear space-charge fields can produce filamentation of the phase-space distribution, resulting in growth of the rms emittances. In addition if the rms size of the beam is mismatched to the periodic focusing lattice, the rms beam size will oscillate. These oscillations can produce an extended beam halo and a large growth of the rms emittance. This halo formation can be understood as a resonant interaction between the oscillating core of the beam and individual particles traveling through the core, and occurs when the particle frequency is about half the core frequency.

The importance of the space-charge force in a linac can be measured by the tune-depression ratios, one for each plane. To define the tune depression for a given plane, we first define σ_0 as the phase advance per focusing period of single particles as undergoing betatron motion in the limit of zero beam current; σ_0 is a measure of the strength of a linear external focusing force. Another important quantity σ is defined to represent the phase advance per focusing period at full current. Strictly speaking there is not a unique value for σ because the space-charge force is generally not linear. A useful definition of σ that provides a unique value is obtained by replacing the real beam with an equivalent uniform beam with the same second moments as the real beam. The tune-depression ratio is defined as σ/σ_0. The extreme values $\sigma/\sigma_0 = 0$ and 1, represent the space-charge dominated and emittance-dominated limits, respectively. For a high current proton linac, the tune-depressions typically range between about $0.5 \leq \sigma/\sigma_0 \leq 0.9$.

In circular machines it is customary to measure the importance of space charge by a tune shift $\Delta\nu = \nu - \nu_0$, rather than the ratio that we use in linacs. This makes sense because in circular machines the current is limited by machine resonances that depend on the tune ν. To compare the parameters σ and ν, we note that $\nu_0 = N_p\sigma_0/2\pi$, where N_p is the number of focusing periods in the ring. The quantity ν represents the tune including space charge, and if this is defined as $\nu = N_p\sigma/2\pi$, where σ is defined in terms of the equivalent uniform beam, we find that

$\sigma/\sigma_0 = 1-|\Delta\nu|/\nu_0$ $\sigma/\sigma_0 = 1-|\Delta\nu|/\nu_0$. Suppose we substitute $|\Delta\nu| = 0.25$, which is a conservative rule of thumb for an acceptible maximum space-charge tuneshift, and choose a value for the zero-current tune ν_0=5.75 that is close to the design value for the SNS ring. Then we find that σ/σ_0=0.95, which is not much tune depression by linac standards. This shows that the beam in a ring is in the emittance-dominated regime, and suggests that most direct space-charge effects that are observed in linacs should be relatively less important for beams in rings. Another way to look at this is to say that it takes very little space charge in the ring before you begin to have problems. One other implication of this result is that the equilibrium beam distribution in the ring will be expected to have a Gaussian-like profile, because for an emittance-dominated beam the Debye length, which is the length scale over which the beam density falls to zero, is large compared with the rms beam size.

Next let's return to the subject of space-charge effects in the linac. In a proton linac the beam quality is degraded by space-charge-induced emittance growth. These emittance growth effects can be separated into four general categories. First is the charge redistribution effect, which is the main cause of emittance growth in rms-matched nonequilibrium beams, when there is a change in the focusing lattice. For this mechanism the emittance grows very rapidly within one-quarter plasma period with an associated transfer of space-charge field energy to particle kinetic energy as the charge redistributes to balance the forces within the beam. Second is kinetic energy transfer between planes, which is caused by a tendency of beams to reduce large thermal asymmetries between planes defined by the focusing elements. This mechanism usually has a time scale of tens of plasma periods. Third is emittance growth caused by mismatch of the rms beam ellipse to the acceptance of the periodic focusing lattice. This mechanism derives its free energy for the initial potential energy associated with imbalance between the external focusing force and the defocusing forces associated with space charge and emittance; a typical time scale is tens of plasma periods. There is a fourth category of emittance growth caused by envelope instability in a periodic channel when the focusing force is too strong. This mechanism can be avoided by requiring that σ_0<90°.

In practice the rms mismatched case supplies the most free energy for emittance growth and this growth can lead to a significant extended beam halo. The beam halo that is observed in 2D phase-space projections may appear either as a phase-space structure in the form of filaments or rings, or it may be a relatively featureless

extension of the beam density. In 2D transverse phase-space projections of a 3D bunch the filaments that form from the effects of the nonlinear space-charge force often project into a smooth featureless halo distribution. The physical mechanism of emittance growth and halo formation for an rms mismatched beam can be explained as the resulting from the space-charge field from an oscillating beam core, which can resonate with the particles undergoing betatron oscillations. This mechanism has been studied using the particle-core model in which one assumes a linear, uniform focusing channel with a round continuous uniform density beam that is mismatched to excite an azimuthally symmetric breathing mode (see Fig.1). Test particles are launched to represent the individual particles passing through the core. The equations of the model include the round-beam envelope equation to represent the breathing oscillations of the core, and the single particle equation of motion in the field of a uniform density beam for a particle with zero angular momentum, which passes back and forth through the core. One finds that a parametric resonance occurs when the particle oscillation frequency is half the core oscillation frequency [1]. Although the resonant amplitude is self limiting because of the decreasing space-charge force outside the beam, the resonance is nevertheless effective at driving some particles to much larger amplitudes. For a given value of a mismatch parameter, defined as the ratio of the initial beam size to the matched beam size, the resonant amplitudes have a maximum value for a given mismatch, which is set by a separatrix that is observed in a stroboscopic plot of the phase-space motion (see Fig. 2)[2]. By solving the model equations numerically, one finds that the maximum particle amplitude normalized to the rms beam size is insensitive to the tune depression over a wide range of tune depression values. Although the tune depression does not have a strong influence on the normalized maximum amplitude, it does influence the growth time of the halo so that for a beam in the emittance-dominated limit, the time for a resonantly-driven particle to move from a point near the inner separatrix where its amplitude is smallest to the outer separatrix where its amplitude is greatest is much larger than for a beam in the space-charge limit. The model predicts that as the mismatch is turned on, the maximum amplitude rises very sharply at a value of the mismatch parameter equal to unity (see Fig 3), so that according to the model even a few percent of mismatch would result in observable beam halo even for an emittance-dominated beam. Thus, the model predicts that the beam halo from mismatch may be hard to avoid in a real accelerator.

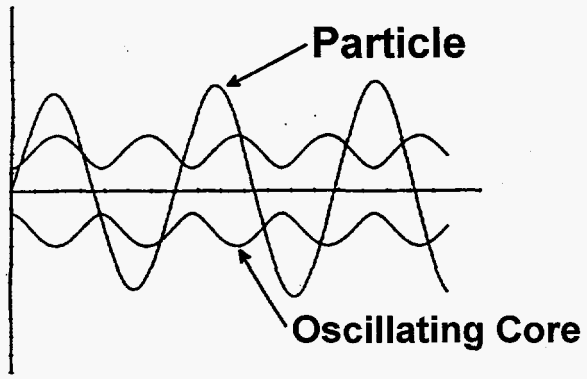

Fig. 1 Transverse oscillations versus time for a particle and an oscillating beam core as represented in particle-core model.

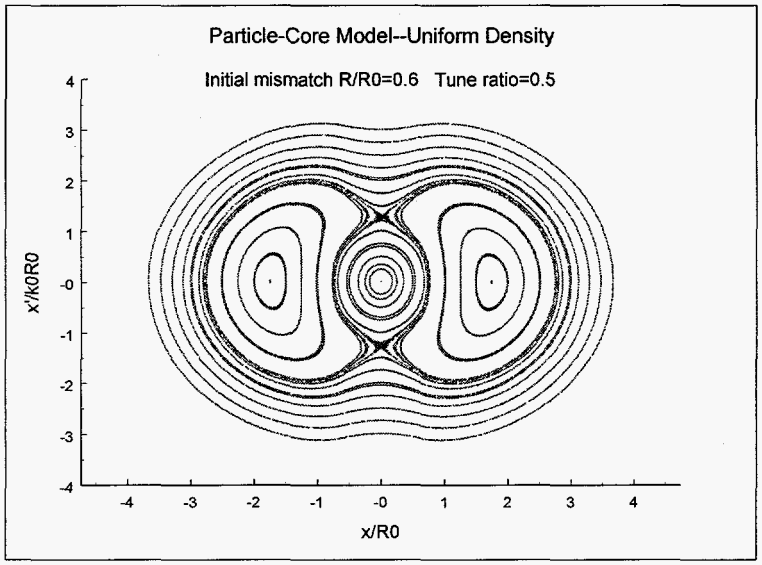

Fig. 2 Stroboscopic plot from the particle-core model of the phase space motion of 32 initial particle coordinates for a tune depression ratio of 0.5 and an initial mismatch (ratio of initial core size to matched core size) of 0.6, showing the central core region, and the resonance region centered on the two stable fixed points. The phase-space motion is strobed each time the core is at its minimum size. The intersection of the outer separatrix with the horizontal axis gives the maximum amplitude for the assumed tune-depression ratio and mismatch value.

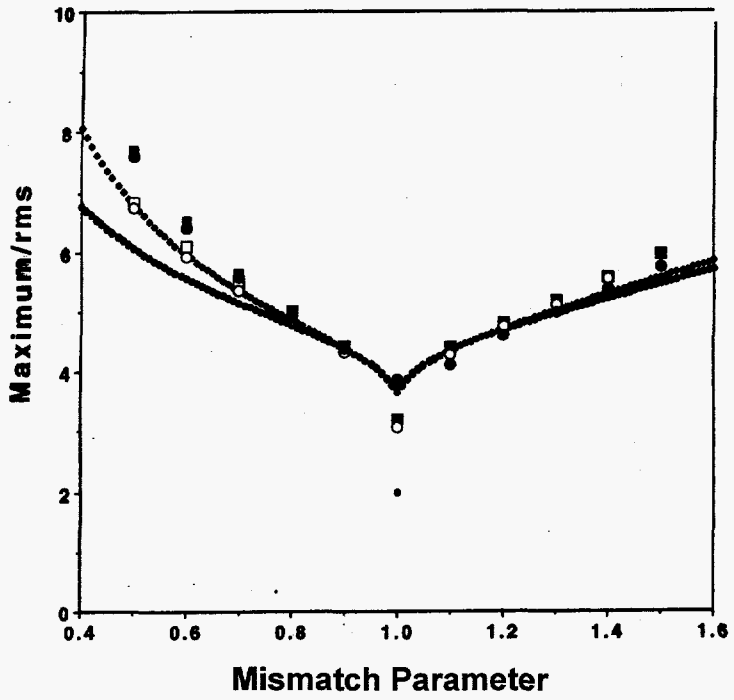

Fig. 3. Ratio of maximum amplitude to rms size versus the mismatch parameter. The curves show the predictions of the particle core model for two tune depression ratios 0.5 and 0.9. The points show the results from numerical simulation for the same two tune ratios and two different initial distributions (Gaussian and thermal).

The numerical solution of the model shows that the maximum amplitude is proportional to the core radius which is approximately proportional to the rms beam size. An analytic solution exists that relates the rms beam size to the beam parameters [2], and from this we obtain a scaling formula for the maximum amplitude of resonantly driven halo particles. The scaling formula predicts that for a given initial mismatch, the maximum amplitude increases with increasing initial rms emittance, and decreases with increasing bunch length, increasing bunch frequency, and increasing focusing strength.

The design principles for a high-current proton linac are strongly influenced by the need to control the space-charge effects that we have discussed. For pulsed linac injectors to rings, the main requirement is usually the need to provide linac output emittances that are safely within the acceptance of the ring. For CW linacs the requirement is usually based on the need to limit the beam losses in the linac. For

energies above about 100 MeV the beam losses should be limited to at least a few watts per meter of lost beam power. As a general rule strong focusing should be provided in all three planes. It is desirable to avoid abrupt changes in the focusing strength that could lead to beam mismatch. If transitions such as to a new focusing lattice or a new frequency can not be avoided, beam matching should be provided. Beam matching requires adjusting the focusing strengths to make the Courant-Snyder parameters of the injected beam equal to the matched values for the periodic focusing lattice. The matching can be made nearly independent of beam current if σ_0/L, where L is the focusing period, is the maintained the same on both sides of the transition. Choosing higher frequency can reduce space-charge effects by distributing the total beam charge over more bunches and by increasing the longitudinal focusing strength. The frequency choice is generally limited by transverse and longitudinal acceptances.

Finally, we summarize some characteristics of proton beams in rf linacs that are often different than for beams in circular machines. Bunches in linacs are nearly spheroidal with aspect ratios that are not far from unity; linac bunches are also usually longer than their transverse sizes. The bunch dimensions in rf linacs are usually small compared with the aperture radius, and as long as the beam is relatively well aligned, the image forces from charges induced in the walls are usually small in linacs compared with the direct space-charge force. The linac beam passes through no dipole magnets, and linac beams are not subject to resonances caused by periodic sampling of the same errors as in circular machines. Consequently, more highly depressed tunes are possible in linacs. The linac beam spends only a few microseconds in the linac, so linac beams usually do not attain thermal equilibrium.

3. Practical Calculation of Linac Space Charge Forces

Because of the complexity of the space-charge force, calculation of space charge effects by analytic methods are of limited value and computer codes are necessary. Fortunately, the rapid progress in computer capability in the past 20 years has increased the number of particles that can be traced through the linac from 10^3 to 10^7. The simplest space-charge programs are those which replace the actual beam distribution with an equivalent uniform beam that has the same second moments as the real beam. This type of code traces the beam envelope and is especially useful for beam-matching optimization. However, to represent the full nonlinear space-charge force that is responsible for emittance growth and halo formation, multiparticle simulation methods are generally used. Although it is not practical to model the

interparticle Coulomb collisions for the full 10^9 particles in a real linac bunch, representing these collisions by a smoothed space-charge potential and tracking a smaller number of macroparticles is a good approximation. We use the particle-in cell (PIC) method, in which at each step a mesh is superimposed on the bunch to smooth the space-charge fields. This reduces the effects of artificially large forces that would otherwise be caused by binary encounters between macroparticles. Computer simulation runs are carried out with up to about 10^5 macroparticles on personal computers, and 10^7 macroparticles on high performance parallel processor computers. SCHEFF, a 2D PIC code, is still the most commonly used space-charge routine for proton linac simulations. Recently we have begun using a 3D PIC code.

The objective of the simulation runs with numbers as large as 10^7 particles is to obtain better statistical precision especially for the outer parts of the beam distribution. Running 10^7 particles using 128 processors on a 64X64X128 grid takes about 5.5 hours. Comparison was made between the SCHEFF and 3D PIC simulations of the 1.7-GeV proton-linac design for accelerator production of tritium. Excellent agreement for both the rms sizes and emittances and for the maximum particles was obtained for runs of 10^5 macroparticles using a 20X40 grid for SCHEFF and a 32X32X64 grid for the 3D PIC subroutine.

4. Experimental Studies of the LANSCE Linac

Next we describe the study of the LANSCE (formerly known as LAMPF) linac carried out by Garnett, Mills, and Wangler in 1989 [3], which has been continued and improved by recent work of F. Merrill and L. Rybarcyk[4]. A block diagram of the linac is shown in Fig.4. The studies involved simulation of the LANSCE beam and comparison of the simulation results with beam measurements. The objective was to compare the predictions of the simulation code with experimental results. Perhaps the most important part of the study was to determine the 6D input beam distribution at the drift-tube linac input. Measurements of beam current, transverse beam profile and transverse emittance were available in the low-energy beam transport (LEBT) upstream of the DTL, and these measurements were used to determine the transverse beam characteristics. The longitudinal properties of the injected beam were determined by simulation of the bunching through the fields of the buncher cavities. Typical results are shown in Fig.5. The space-charge force causes a noticeable distortion of the phase-space distributions at the input. Partial neutralization of the beam charge occurs through collisional ionization of the residual gas, and the

effective current was determined by choosing the value that best fits the measured rms beam sizes. Table 1 shows the comparison of simulations with measurements for the transverse emittances at 100 and 800 MeV, the rms beam size at 100 MeV, the bunch width at 121 MeV. The width is determined by sweeping the phase of the cavity to move the longitudinal rf separatrix through the beam bunch and using an absorber and collector to measure the energy gain difference between the accelerated and non-accelerated beam. Finally the integrated particle loss along the coupled-cavity linac (CCL) was compared with the integrated loss obtained from the current monitors. The error in the measured emittance at 100 MeV is obtained from the difference between the two measurements, one from a wire-scan method and one from a slit and collector method. Error estimates for the other measurements were not available. Errors applied to the simulated quantities were based on the differences between results for a range of different assumptions about the charge neutralization and component parameter values in the LEBT. With the exception of the particle loss, the simulation results were in fairly good agreement with the measurements. We found that the magnitude of the particle loss prediction from simulation had a large uncertainty, which we believe is a result of the uncertainties associated with the population of the tail in longitudinal phase space that is caused by the bunching process.

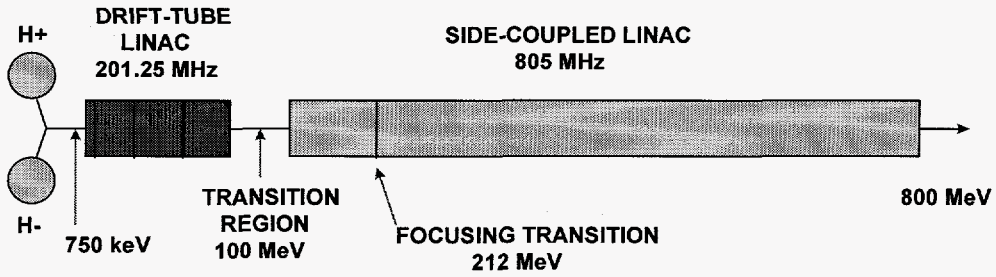

Fig. 4. Block diagram of the LANSCE proton linac at Los Alamos.

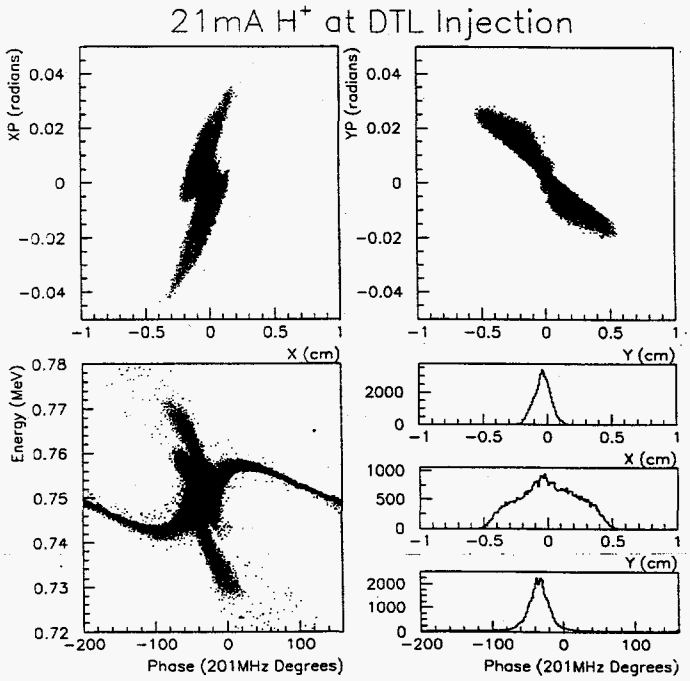

Fig. 5. Phase-space distributions and projections at the drift-tube linac input from simulation of the bunching process in the LANSCE linac.

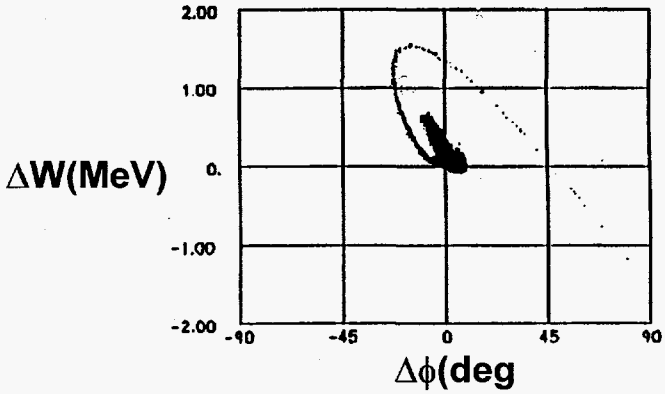

Fig. 6. Longitudinal phase space at 100 MeV from a simulation of the LANSCE linac.

Table 1 Comparison of Measurements with Simulation of the LANSCE Linac.

Quantity	Measurement	Simulation
$\varepsilon_{rms,n}$ (mm-mrad) at 100 MeV	0.40±0.14	0.29±0.03
$\varepsilon_{rms,n}$ (mm-mrad) at 100 MeV	0.71	0.65±0.02
x_{rms} (mm) at 800 MeV	5.4	7.0±1.0
Longitudinal separatrix (deg) at 121 MeV	16	20±3
Particle loss (%) at > 100 MeV	~0.1	0.9±0.5

Beam losses above about 100 MeV are the main concern at LANSCE because of the induced radioactivation of the accelerator, which inhibits maintenance on the machine. The experimental distribution of losses along the CCL can be approximately obtained from activation measurements made after the run, together with a model that relates activation with beam losses versus energy. The locations of the two main beam loss peaks in the CCL near 100 and 212 MeV were well reproduced by the simulations. From the simulations we are able to explain the beam-loss mechanisms. A first peak near 100 MeV is caused by inadequate matching and transverse acceptance of the focusing lattice. A second peak at about 212 MeV occurs where the transverse acceptance drops as a consequence of a transition where the focusing period doubles. The beam losses at that location are mostly cause by 100 MeV particles that were not captured in the 805-MHz longitudinal buckets at the 100 MeV injection into the CCL. We refer to these as longitudinal losses, and the lost particles are those that are included in the tail in longitudinal phase space caused by the incomplete bunching of the beam injected into the DTL. Other simulation studies were made of the LANSCE linac with an RFQ replacing the first DTL tank. These studies have shown that the longitudinal tails would be almost completely removed by the superior bunching characteristics of the RFQ. A proton linac with an RFQ front end would not be expected to have beam losses from the longitudinal tail. Beam halo could still be produced by mismatch. Detailed and systematic measurements of the outer beam halo after the linac were carried out by H. Koziol [5] in 1975, using a movable plate and beam-loss scintillation monitors to detect the scattered radiation from the plate. However, machine time was never made available to make comparable halo measurements in the linac.

5. Conclusions

In this paper we have discussed space-charge effects from the linac viewpoint. The space-charge force in a linac produces limiting currents, emittance growth that degrades the beam quality, and beam halo. We discussed the impressive advances in computing capability that have allowed us to simulate space-charge effects in a linac; the number of macroparticles that can be traced through the linac has increased in recent years from about 10^3 to 10^7. Also, excellent agreement is found between the main space-charge routines. This simulation capabilility gives us more confidence to describe the details of the beam distribution including the beam halo for a linac design that includes realistic errors. Experimental studies of the LANSCE linac reveal the complexity of the effects in a realistic linac and shows how they affect the beam distribution. We find that there is good agreement between beam simulation and LANSCE beam measurements for the rms quantities, the maximum beam size and the relative beam-loss distribution. Further progress can be made if we can obtain more experimental measurements of beam halo in the linac itself.

References

[1] R. L. Gluckstern, Phys. Rev. Lett. 73(1994) 1247.

[2] T. P. Wangler, E. R. Gray, S. Nath, K. R. Crandall, and K. Hasagawa, "New High Power Linacs and Beam Physics", Presented at the 1997 Particle Accelerator Conference, Vancouver, May 12-16, 1997.

[3] R. W. Garnett, R. S. Mills, and T. P. Wangler, " Beam Dynamics Simulation of the LAMPF Linear Accelerator", Proc. Of 1990 Linear Accelerator Conf., Sep. 10-14, 1990, Los Alamos Report LA-12004-C, pp 347-350.

[4] Frank Merrill and Lawrence J. Rybarcyk, " Transverse Match of High Peak-Current Beam into the LANSCE DTL Using PARMILA", Proc. of XVIII International Linear Accelerator Conf., Aug. 26-30, 1996, CERN report CERN 96-07, pp 231-233.

[5] H. Koziol, "Halo Measurements on the LAMPF 800 MeV Beam", Los Alamos MP-Division Report MP-3-75-1.